Environmental Science and Pollution Research (2018) 25:32540–32548
https://doi.org/10.1007/s11356-018-3105-9

RESEARCH ARTICLE

Green synthesis of silver and gold nanoparticles using *Stemona tuberosa* Lour and screening for their catalytic activity in the degradation of toxic chemicals

Bodaiah Bonigala[1] · Bhushanam Kasukurthi[1] · Vinay Viswanath Konduri[1] · Usha Kiranmayi Mangamuri[2] · Rosaiah Gorrepati[2] · Sudhakar Poda[1]

Received: 8 January 2018 / Accepted: 29 August 2018 / Published online: 20 September 2018

Abstract

In the present study, silver and gold nanoparticles (AgNPs and AuNPs) were green synthesised using the aqueous plant extract of *Stemona tuberosa* Lour. When plant extract was mixed with $AgNO_3$ and $HAuCl_4$ solutions in separate reactions, the amalgamated solutions turned deep reddish brown and dark purple in colour after 48 h indicating the formation of AgNPs and AuNPs. UV-Visible analysis of green synthesised AgNPs and AuNPs have shown absorption maximum at 443.85 nm and 539.72 respectively after 48 h. Energy dispersive X-ray spectroscopy (EDX) analysis confirmed the presence of pure silver in the green synthesised AgNPs and pure gold in the plant-mediated AuNPs. X-ray diffractometer (XRD) data revealed the face-centred cubic nature of AgNPs. Fluorescence transmission infrared (FTIR) spectrum has shown the characteristic peaks of different phytochemicals in the plant extract which acted as stabilising or capping agents of AgNPs. Scanning electron microscopy (SEM) analysis of AgNPs and AuNPs revealed that the nanoparticles are monodispersed. Transmission electron microscopy (TEM) studies revealed that AgNPs were mostly spherical with an average size of 25 nm whereas selected area electron diffraction (SAED) analysis confirmed their crystalline nature. Both AgNPs and AuNPs of *S. tuberosa* Lour have shown potential catalytic activity in the presence of sodium borohydride ($NaBH_4$) in the degradation and removal of 4-nitrophenol, methylene blue, methyl orange and methyl red.

Keywords Green synthesis · *Stemona tuberosa* Lour · AgNPs · AuNPs · Catalytic activity

Introduction

Biosynthesis is a novel technique for metallic nanoparticles synthesis and emerged as a major research area in the field of nanobiotechnology. It gained prominence over physical and chemical methods due to its cost-effective and ecofriendly nature (Ahmed et al. 2016). Moreover, biosynthesized metallic nanoparticles were shown to exhibit high yield and high stability (Saha et al. 2017). In the present decade, the scientists and young researchers are showing special enthusiasm towards plant-mediated synthesis (green synthesis) of metallic nanoparticles because it is a simple and time-saving process than other biological methods, i.e. microbial cultures. In addition, green-synthesised nanoparticles have shown significant antimicrobial, anticancer and pesticidal activities in vitro (Swamy et al. 2015). Recent literature suggests that platinum, gold and silver nanoparticles are mostly used in soaps, shoes, detergents, shampoos, toothpaste and cosmetics in addition to medical and pharmaceutical applications (Tahir et al. 2015).

In the twenty-first century, both developed and developing countries are encouraging rapid industrialisation to serve the needs of growing human population. Establishment of vast number of industries leads to environmental pollution with the release of toxic chemicals into water and air. The hazardous pollutants have shown to exhibit negative impact on human health and other living organisms which finally leads to ecological imbalance (Kjellstrom et al. 2006). 4-Nitrophenol is a synthetic, phenolic and polymorphic chemical often used

Responsible editor: Philippe Garrigues

✉ Sudhakar Poda
sudhakarpodha@gmail.com

[1] Department of Biotechnology, Acharya Nagarjuna University, Nagarjunanagar, Guntur, Andhra Pradesh 522510, India

[2] Department of Botany and Microbiology, Acharya Nagarjuna University, Guntur, Andhra Pradesh 522510, India

in pharmaceutical industry in the manufacture of drugs. It is also used in the leather industry to darken the leather as well as in the manufacture of fungicides, insecticides and synthetic dyes. The remnant of 4-nitrophenol from industrial waste water when mixed with water bodies leads to pollution and cause health problems to living organisms (Edison and Sethuraman 2013). Organic dyes are synthetic chemicals which imparts colour when binds to a material. Methylene blue is a cationic dye, synthetic heterocyclic aromatic chemical and dark green powder when dissolved in water turns into blue colour. It is used in textile and paper industries for coloration of fabrics and paper (Ansari et al. 2011). Methyl orange and methyl red are synthetic azo dyes and widely used in textile, paper, leather and food industries as colouring agents (Kamlesh Shah 2014). About 15% of these non-biodegradable and toxic dyes are lost in the dyeing process and released into industrial effluents. The removal of synthetic organic chemicals from waste water is an essential environmental issue because they cause serious health issues in humans and other living organisms when ingested (Sudha et al. 2014). The complete removal of these dyes from waste water by physical and chemical methods requires high technology which is not cost-effective and consumes more energy (Kharub 2012).

Waste water treatment for degradation and removal of toxic organic pollutants by metallic nanoparticles is a novel approach and an alternative to physical and chemical methods. According to current research findings, green-synthesised metal nanoparticles have exhibited potential catalytic activity in the degradation and removal of toxic synthetic organic chemicals (Vidhu and Philip 2014; Reddy et al. 2016; Karthik et al. 2016). *S. tuberosa* Lour is an herbaceous plant, commonly known as wild asparagus and belongs to the family *Stemonaceae*. The plant is seen in China, Taiwan and in India, the roots of the plant contains alkaloids and used in the treatment of jaundice, tuberculosis, cough, scabies and gynaecological disorders in different parts of the world (Bharali et al. 2014). The present study aims at AgNP and AuNP synthesis using aqueous extract of *Stemona tuberosa* Lour. The biosynthesized AgNPs and AuNPs were used as catalyst in degradation and removal of 4-nitrophenol, methylene blue, methyl orange and methyl red by $NaBH_4$.

Materials and methods

Collection of the plant material

The aerial parts of *Stemona tuberosa* Lour were collected from Tirumala hills, Tirupathi, Andhra Pradesh, India. The plants were taxonomically identified and authenticated by Prof. M. Vijayalakshmi, Dean and Professor, Dept. of Botany and Microbiology, Acharya Nagarjuna University, Guntur, Andhra Pradesh, India.

Preparation of the aqueous plant extract

The plant material collected was washed thrice with distilled water to remove the dust and dried under the shade to remove the moisture. The dried plant material was then cut into pieces and crushed into fine powder with a suitable pulveriser. To 100 ml of molecular grade water, 3 g of finely crushed dried powder was mixed, boiled at 100 °C for 10 min and the extract was filtered with Whatman No. 1 filter paper to remove impurities.

Green synthesis of AgNPs and AuNPs from the extract of *Stemona tuberosa* Lour

Of the filtered plant extract, 2 ml, 5 ml, 10 ml, 15 ml and 20 ml were added to 198 ml 195 ml, 190 ml, 185 ml and 180 ml of 1 mM silver nitrate ($AgNO_3$) solution and kept for incubation. The effect of $AgNO_3$ concentration on AgNP formation was analysed by adding 10 ml of plant extract to 190 ml of 0.1 mM, 0.5 mM, 1 mM, 1.5 mM and 2 mM concentrations of $AgNO_3$ in separate reactions. Later, the suspension was kept for incubation at room temperature. Whereas to synthesise AuNPs, 1 ml of *S. tuberosa* aqueous extract was added to 49 ml of 0.5 mM gold (III) chloride trihydrate ($HAuCl_4$) solution and kept for incubation at room temperature. The change in the colour of amalgamated solutions was observed after 48-h incubation.

Characterisation of plant-mediated AgNPs and AuNPs

The formation and stability of AgNPs and AuNPs using *S. tuberosa* Lour extract was confirmed by UV-Visible spectroscopic studies after 48 h using $AgNO_3$ and $HAuCl_4$ solutions as blank respectively and the values were recorded within the range of 200 to 800 nm. To know the effect of time on AgNP and AuNP formation, the amalgamated solutions of 10 ml of plant extract and 190 ml of $AgNO_3$ as well as 1 ml of plant extract and 49 ml of $HAuCl_4$ were analysed using UV-Visible spectrometer for every 1-h time intervals. The plant-mediated AgNPs were examined in HORIBA Z100 zeta potential analyser based on the principle of laser Doppler electrophoresis to know the stability of AgNPs and the measurements were obtained in the range of − 200 to + 200 mV.

The AgNPs and AuNPs were purified by repeated centrifugation of AgNP and AuNP solutions at 10,000 rpm for 15 min. The pellets of both AgNPs and AuNPs were transferred into separate china dishes and kept for shade evaporation. The dried nanoparticles were washed with distilled water, allowed for shade drying and the process was repeated thrice. The purified and dried nanoparticle samples were collected and used for characterisation. Energy dispersive X- ray spectroscopy study was performed to determine the elemental composition of biosynthesized AgNPs and AuNPs with field emission scanning electron microscope equipped with dispersive analysis of

X-rays (EDAX). The purified biosynthesized AgNPs were studied using Philips X'pert pro XRD with an operation voltage of 40 kV and current of 30 mA with CuKα radiation (1.540 °A) between 2θ° angles (30°–80°) for analysing peak data and crystal structure. Fluorescence transmission infrared (FTIR) analysis of the AgNPs was carried out through potassium bromide (KBr) pellet (FTIR grade) method in 1:100 ratio and spectrum was recorded using Jasco FT/IR-6300 FTIR equipped with JASCO IRT-7000 Intron Infrared microscope (JASCO, Tokyo, Japan) using transmittance mode operating at a resolution of 4 cm^{-1} in order to find out the phytochemicals in *S. tuberosa* Lour extract which are responsible for reduction process in the AgNP synthesis. Scanning electron micrographs of the purified and dried AgNPs as well as AuNPs were taken using Zeiss SEM machine. Thin films of the sample were prepared on a glass slide by just dropping a very small amount of the sample on the grid, allowed to dry by placing it under a mercury lamp for SEM images after 10-min drying. Transmission electron microscope study was carried out to know the morphology and particle size distribution of AgNPs. The grid for TEM analysis was prepared by placing a drop of *S. tuberosa* Lour plant-mediated AgNP suspension on a carbon-coated copper grid and allowing the water to evaporate inside a vacuum dryer. The grid containing AgNPs was scanned by a Hitachi Japan Model 7500 TEM machine.

Evaluation of catalytic activity of plant-mediated AgNPs and AuNPs

In the present study, AgNPs and AuNPs of *S. tuberosa* Lour were utilised as catalysts separately in the degradation and removal of 4-nitrophenol, methylene blue, methyl orange and methyl red by $NaBH_4$. The procedure of degradation of a respective synthetic chemical or dye (4-nitrophenol or methylene blue or methyl orange or methyl red) by $NaBH_4$ in the presence of AgNPs or AuNPs as catalyst involves three reactions. All the reactions were studied in Thermoscientific UV-Visible spectrophotometer using Milli-Q water as blank. The first reaction is prepared by adding 1.5 ml of 1 mM of a synthetic chemical or dye to 1.5 ml of Milli-Q water, mixed well and analysed in UV-Visible spectroscopy. Later, 1 mg of solid $NaBH_4$ was added to first reaction to prepare second reaction and analysed in UV-Visible spectroscopy. The third reaction is prepared by adding 20 μl of green-synthesised nanosolution to the second reaction and analysed in UV-Visible spectroscopy after 1 min (Edison and Sethuraman 2013).

Results and discussion

Addition of *S. tuberosa* Lour plant extract with aqueous solution of silver nitrate led to the observable colour change from yellowish to dark reddish brown solution after 48-h incubation (Fig. 1(d)) due to surface plasmon resonance indicating AgNP formation (Syed et al. 2013; Otari et al. 2012). Whereas the amalgamated solution of $HAuCl_4$ and plant extract turned into deep purple colour after 48-h incubation. In general, AuNPs exhibit ruby red to dark purple colour in aqueous solutions due to excitation of surface plasmon vibrations. Thus, the formation of deep purple colour in the reaction mixture indicated the formation of AuNPs (Fig. 1(f)) (Singh et al. 2016).

Characterisation of plant-mediated AgNPs and AuNPs

UV-Visible analysis

The green-synthesised AgNPs (amalgamated solution of 190 ml $AgNO_3$ + 10 ml plant extract) have shown absorption maximum at 443.85 nm (Fig. 2a) in UV-Visible spectroscopic analysis after 48-h incubation (Supraja et al. 2016; Ashraf et al. 2016). But the green-synthesised AuNPs (amalgamated solution of 49 ml $HAuCl_4$ + 1 ml plant extract) were shown to exhibit absorption maximum 539.72 nm (Fig. 2b) in UV-Visible spectroscopic analysis after 48-h incubation (Pei et al. 2017; Patra et al. 2016). The amalgamated solution of 1 ml, 5 ml and 10 of the plant extract showed the formation of AgNP (Fig. 2c). Further, when the amalgamated solutions that were kept for incubation to know the effect of $AgNO_3$ concentration were studied in UV-Visible spectroscopy, AgNP

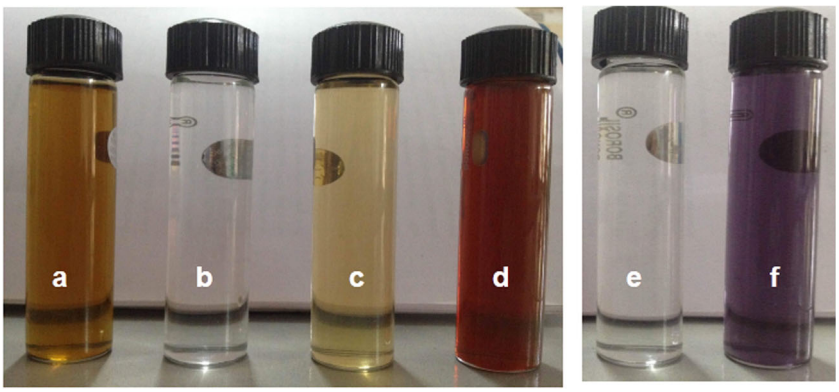

Fig. 1 Green synthesis of AgNPs and AuNPs. (a) Aqueous plant extract. (b) Silver nitrate solution. (c) 1 mM silver nitrate plus plant extract at the start of incubation. (d) AgNPs of *S. tuberosa* Lour. (e) $HAuCl_4$ solution. (f) AuNPs of *S. tuberosa* Lour

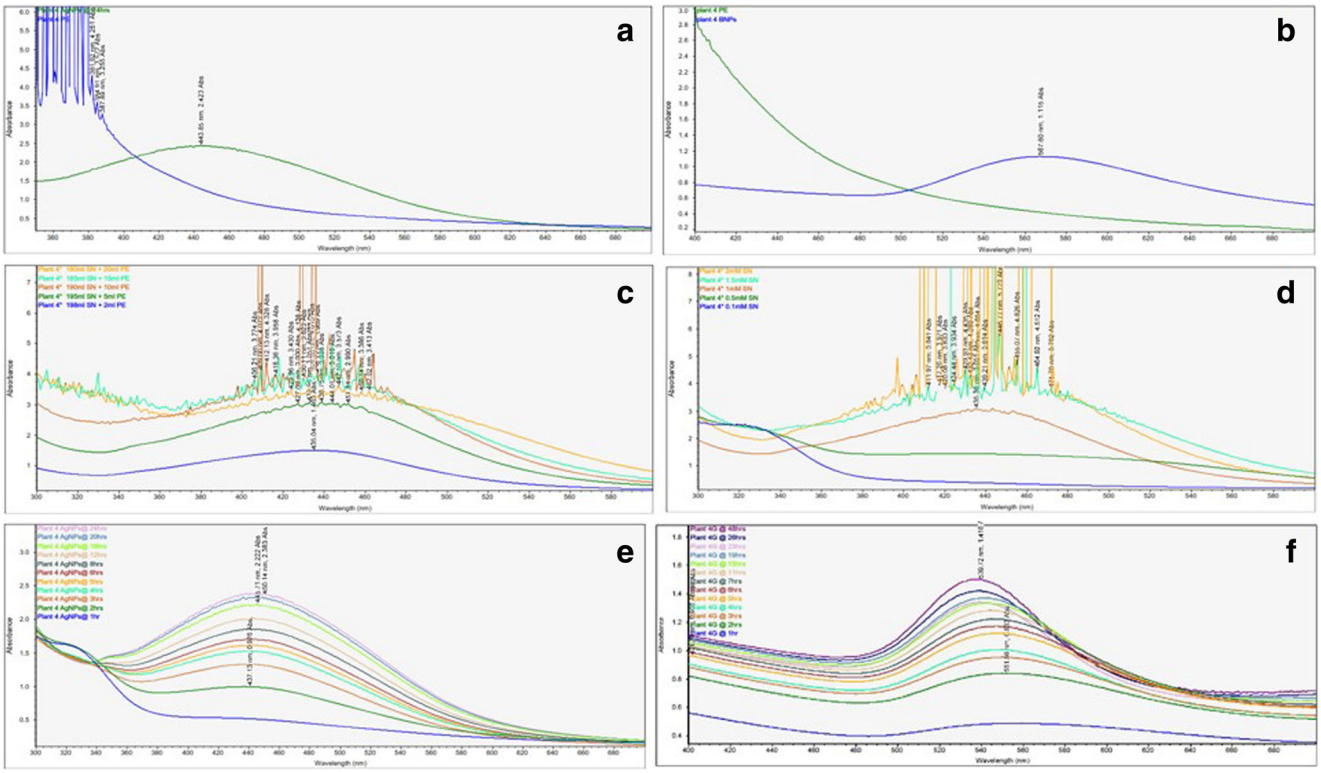

Fig. 2 UV-Visible analysis of *S. tuberosa* Lour. **a** Plant extract and AgNPs. **b** Plant extract and AuNPs. **c** Effect of plant extract concentration on AgNP formation. **d** Effect of $AgNO_3$ concentration on AgNP formation. **e** Influence of time on AgNP formation. **f** Influence of time on AuNP formation. SN silver nitrate solution, PE plant extract, hr time in hours

formation was confirmed in the reactions with only to 0.1 mM, 0.5 mM and 1 mM concentrations of $AgNO_3$ (Fig. 2d). To know the influence of time on AgNP formation, UV-Visible spectroscopic readings were taken to amalgamated solution of 190 ml $AgNO_3$ + 10 ml plant extract at every 1-h time intervals. To know the effect of time on AuNP formation, UV-Visible spectroscopic readings were taken to amalgamated solution of 49 ml $HAuCl_4$ + 1 ml plant extract at every 1-h time intervals. The synthesis of both AgNPs and AuNPs were observed exactly after 2-h incubation as shown in Fig. 2e, f.

Zeta potential analysis

The zeta potential analysis of the charged AgNPs were attracted to oppositely charged electrode and their velocity was measured and expressed in Unit field strength as their mobility. The AgNPs of *S. tuberosa* Lour have exhibited a mean negative zeta potential of − 18.7 mV (Fig. 3a) indicating that the particles are moderately stable and from the data, it can be known that repulsive forces are present among the synthesised AgNPs (Singh et al. 2014; Jyoti et al. 2016).

XRD analysis

X-ray powder diffraction spectrum of green-synthesised AgNPs have shown Bragg peaks (angle 2θ) at 27.81°, 32.24°, 38.17°, 46.24°, 54.82°, 57.51°, 64.50° and 77.44° which corresponds to the indexed planes of 210, 122, 111, 200, 142, 241, 220 and 311 miller indices of face centred cubic (FCC) structure of a regular silver crystal (Ajitha et al. 2014). Using Debye-Scherrer equation, the average particle size of biosynthesized was determined [$d = K\lambda / \beta \cos \theta$] where '$d$' is the mean diameter of the particle; 'K' is the shape factor (0.9); 'λ' is the X-ray radiation source (0.154 nm); 'β' is (π / 180) × FWHM and 'θ' is the Bragg angle. The average particle size of *S. tuberosa* Lour AgNPs was obtained as 28.88 nm and the XRD pattern (Fig. 3b) was in agreement with earlier XRD reports of green-synthesised AgNPs (Jayaseelan and Rahuman 2011; Suresh et al. 2014).

SEM/EDX spectrum study

The EDX spectrum showed highest peak at 3 keV for purified plant-mediated AgNPs and 2.15 keV for the plant-mediated AuNPs and the results were depicted in the Fig. 3c, d. The other peaks present in both the figures are to the protein capping over the AgNPs and AuNPs or may be the element composition of glass that holds the samples or the other elements in the respective salts. The above results were quite similar with the previous reports of biosynthesized AgNPs and AuNPs (Raja et al. 2017; Singh et al. 2016; Tahir et al. 2015).

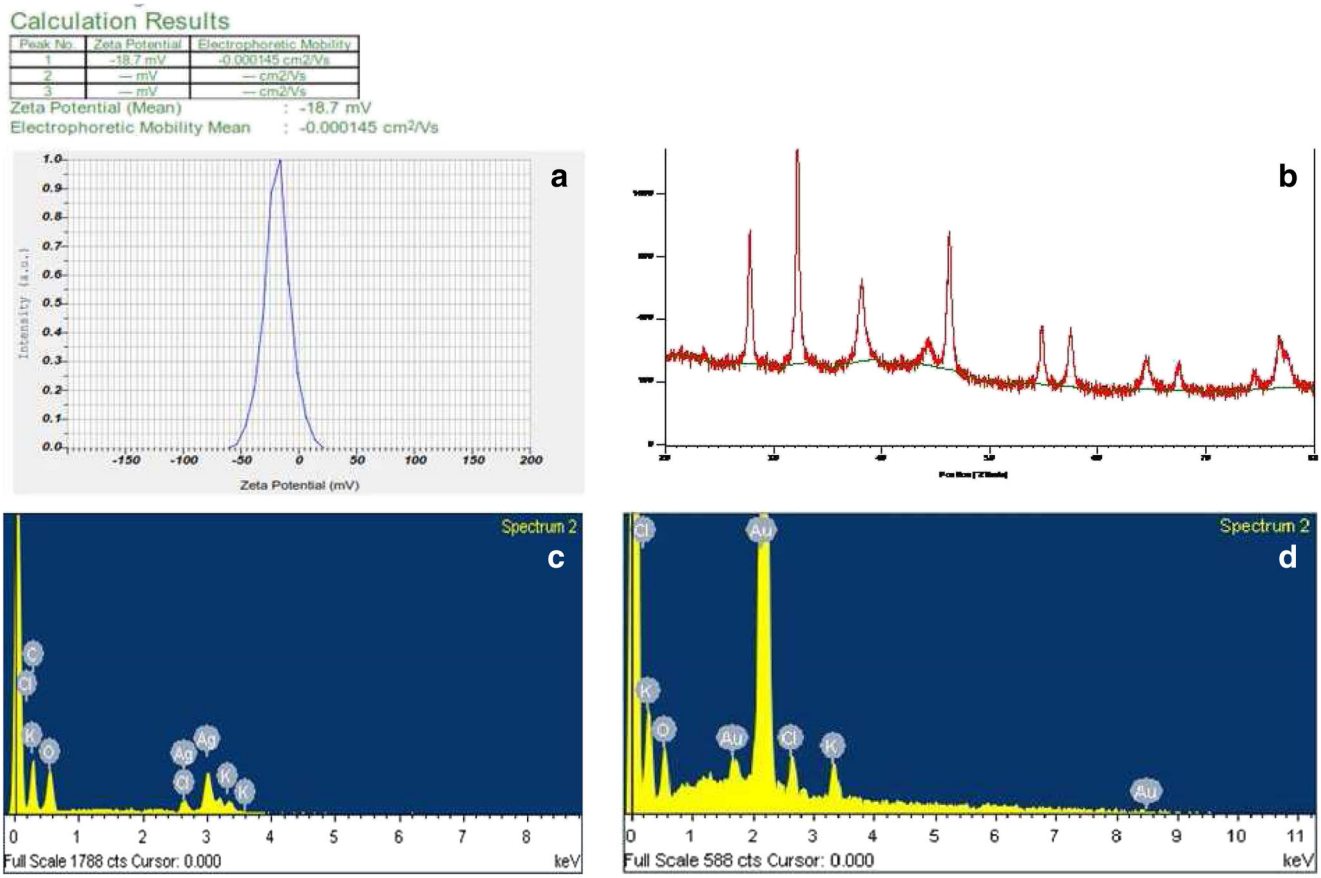

Fig. 3 **a** Zeta potential analysis. **b** XRD spectrum. **c** EDX spectroscopic study of *S. tuberosa* Lour AgNPs. **d** EDX spectroscopic study of *S. tuberosa* Lour AuNPs

SEM and TEM studies

The SEM analysis revealed that AgNPs were spherical to irregular in shape. The SEM images also revealed that AgNPs were not aggregated and mean diameter was found to be 10–12 nm (Fig. 4a) (Shanmugam et al. 2016). The SEM image of AuNPs (Fig. 4d) indicates that the particles were irregular in shape with the mean diameter in the range 20–30 nm (Lee et al. 2015). The TEM images revealed that most of the AgNPs were spherical in shape with an average size of 25 nm (Fig. 4b, c) and is in agreement with results produced in XRD analysis (Padalia et al. 2015). SAED images taken by the TEM machine (Fig. 4e) have shown clearly the crystalline nature of the biosynthesized AgNPs (Jyoti et al. 2016).

FTIR study

The biosynthesized AgNPs displayed a number of peaks in the FTIR spectrum (Fig. 4f) and portrayed the complex nature of particles. The strong and broad peak at 3384.14 cm^{-1} was formed because of O–H bond stretching of alcohols and phenols (Kumar et al. 2016). The peaks formed at 2929.87 cm^{-1} and 2888.51 cm^{-1} due to the characteristic stretching vibrations of C–H stretch and C–H rock of alkanes. The weak peak formed at 2397.52 cm^{-1} was may be the stretch of alkynes. The peaks formed at 1762.94 cm^{-1} and 1714.72 cm^{-1} represents C=O stretch of ketones. The medium and strong peak at the 1620 cm^{-1} is the N–H stretching vibrations of amides (Syed et al. 2013). The $–(CH_3)_3$ bend of alkanes and alkyl groups formed a medium peak at 1390.39 cm^{-1}. The peaks at 1099 cm^{-1} and 1051 cm^{-1} were formed due to the C–O stretch of alcohols. The C–Cl stretch of alkyl halides formed a strong peak at 823 cm^{-1}. These shifts in peak positions reveal that different phytochemicals were present in the plant extract of *S. tuberosa* Lour and hence it can be concluded that bioorganic compounds present in the plant extract acted as reducing and stabilising agents in the AgNP formation (Monali et al. 2009).

Catalytic activity of *S. tuberosa* Lour AgNPs and AuNPs

The synthetic chemical or dye degradation reactions were monitered and depicted in the following order 4-nitrophenol, methylene blue, methyl orange and methyl red. All reactions were analysed by UV-Visible spectrophotometer.

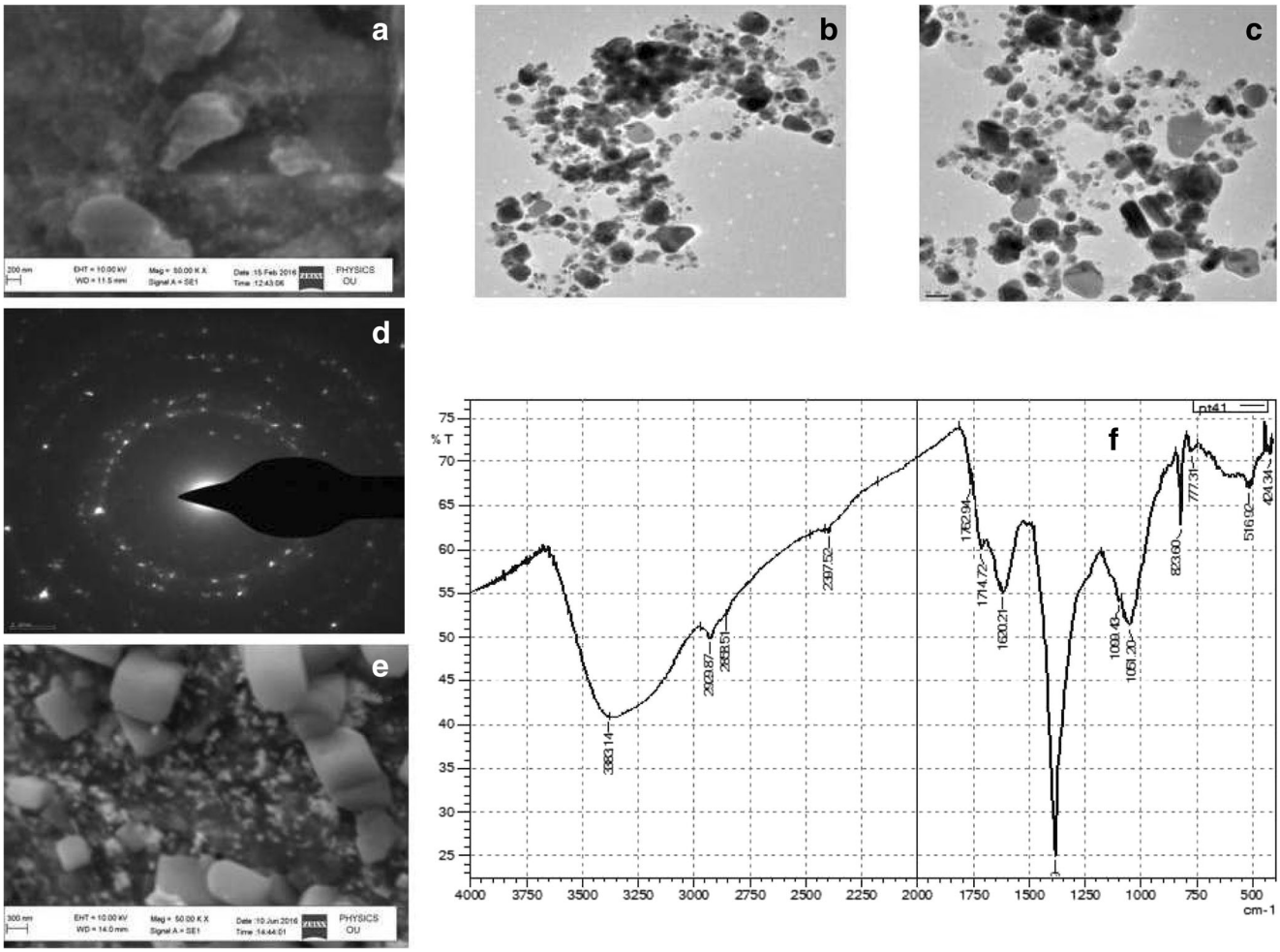

Fig. 4 **a** SEM image of *S. tuberosa* Lour AgNPs. **b**, **c** TEM images of *S. tuberosa* Lour AgNPs. **d** SAED image of *S. tuberosa* Lour AgNPs. **e** SEM image of *S. tuberosa* Lour AuNPs. **f** FTIR spectrum of *S. tuberosa* Lour AgNPs

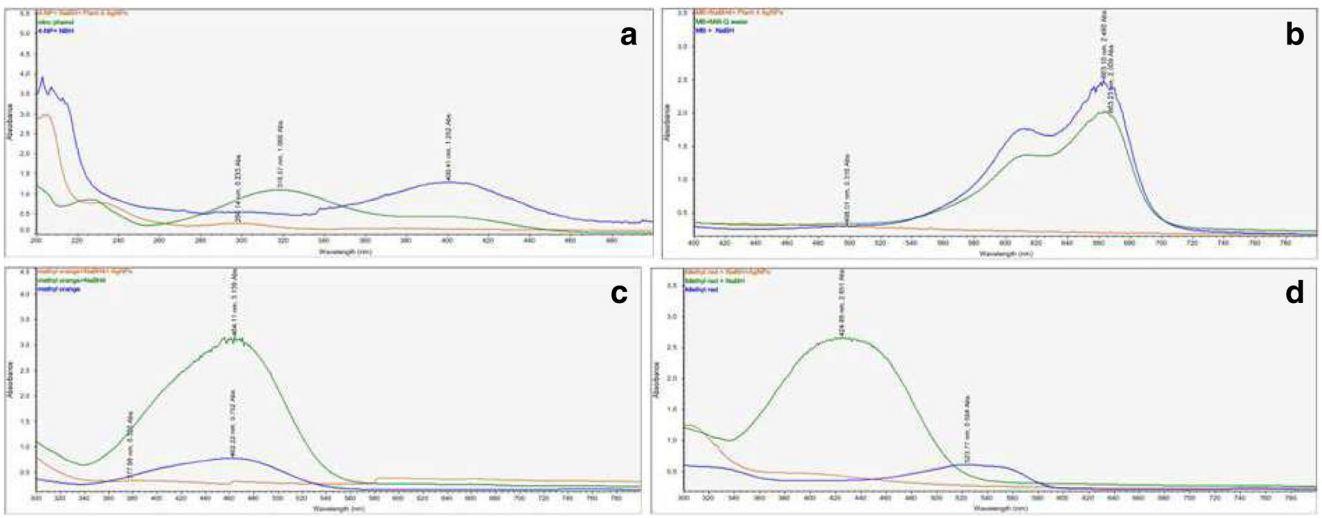

Fig. 5 Catalytic activity of *S. tuberosa* Lour AgNPs on **a** 4-nitrophenol, **b** methylene blue, **c** methyl orange and **d** methyl red. NaBH sodium tetra borate, AgNPs silver nanoparticles

Reduction reactions of 4-nitrophenol

UV-Visible analysis of 4-nitrophenol degradation using $NaBH_4$ with *S. tuberosa* Lour AgNPs and AuNPs as catalysts were shown in Figs. 5a and 6a. The reaction of 4-nitrophenol when monitored in spectrophotometer the absorption maximum 1.252 was observed at 318 nm. In addition of $NaBH_4$ to the first reaction, the solution appeared bright yellow in colour because of the formation of sodium phenolate, no change in the absorption maximum with respect to time was observed and shifted to 400 nm (Prasad et al. 2015). With the addition of plant-mediated AgNPs, the solution turned colourless and the absorption maxima suddenly decreased from 1.252 to 0.233. With the addition of AuNPs to second reaction the solution turned colourless whereas the absorption maximum decreased from 1.252 to 0.360. The above results confirmed that both AgNPs and AuNPs of *S. tuberosa* Lour completely degraded the synthetic chemical 4-nitrophenol (Karthik et al. 2016; Khan et al. 2017).

Reduction reactions of methylene blue

The degradation and removal of methylene blue by $NaBH_4$ in the presence of biosynthesized AgNPs and AuNPs as catalyst were analysed and the UV-Visible results were illustrated in Figs. 5b and 6b. For pure 1 mM methylene blue, absorption maximum of 2.48 was initially observed at 664 nm. When 1 mg of $NaBH_4$ was added, the absorption maximum was recorded at same wavelength with a slight change. With the addition of green-synthesised AgNPs, the solution turned colourless and the absorption maximum was completely decreased from 2.48 to 0.316 indicating that methylene blue was completely degraded (Joseph and Mathew 2015). When biosynthesized AuNPs were added to the second reaction, the solution turned colourless whereas the absorption maximum decreased from 2.48 to 0.064 indicating that methylene blue was completely degraded (Suvith and Philip 2014).

Reduction reactions of methyl orange

Figures 5c and 6c illustrate the results related to the degradation and removal reactions of methyl orange by $NaBH_4$ in the presence of *S. tuberosa* Lour AgNPs and AuNPs as catalysts. In UV-Visible analysis for pure methyl orange, the absorption maximum was found to be 0.752 at 462.22 nm and when 1 mg of $NaBH_4$ was added, the absorption maximum was found to be 3.124 at 461.11 nm. After adding AgNPs, the solution turned colourless with decrease in absorption maxima from 3.124 to 0.320. In the case of AuNPs, the solution turned colourless and the absorption maximum decreased from 3.124 to 0.134. The results clearly indicate that AgNPs and AuNPs completely degraded methyl orange (Sandeep et al. 2016; Varadavenkatesan et al. 2016; Ul Haq Khan et al. 2017) (Tables 1 and 2).

Reduction reactions of methyl red

The UV-Visible analysis results related to the reduction reactions of methyl red by $NaBH_4$ in the presence of AgNPs as well as AuNPs were illustrated in Figs. 5d and 6d. An absorption maximum of 0.558 was observed at 523.77 nm to pure 1 mM methyl red. After addition of 1 mg $NaBH_4$, the absorption maximum of 2.651was obtained at 424.89 nm. With the addition of *S. tuberosa* Lour AgNPs, yellow-coloured solution turned colourless and zero absorption maximum was recorded in the third reaction indicating the complete reduction of methyl red (Jyoti and Singh 2016). In the reaction of AuNPs, the solution also turned colourless but the absorption maximum

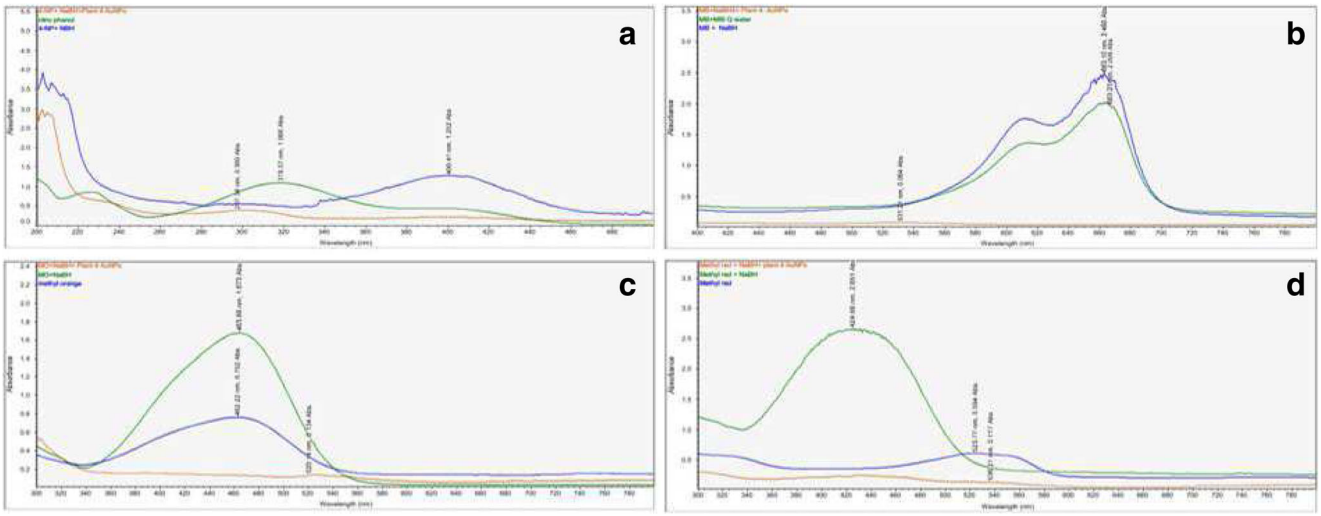

Fig. 6 Catalytic activity of *S. tuberosa* Lour AuNPs on **a** 4-nitrophenol, **b** methylene blue, **c** methyl orange and **d** methyl red. NaBH sodium tetra borate, AuNPs gold nanoparticles

Table 1 Absorption maxima of synthetic chemicals before and after addition of *S. tuberosa* Lour AgNPs

S. no.	Synthetic chemical	Absorption maximum	
		Before the addition of AgNPs	After the addition of AgNPs
1	4-Nitrophenol	1.252	0.233
2	Methylene blue	2.480	0.316
3	Methyl orange	0.752	0.320
4	Methyl red	2.651	Nil

decreased from 0.558 to 0.117 indicating the complete degradation of methyl red (Sinha and Ahmaruzzaman 2015).

Conclusion

Biosynthesis is a reliable technique than physical and chemical methods to synthesise metallic nanoparticles because of its simple, cost-effective and ecofriendly nature. The AgNPs and AuNPs were synthesised by green method using the aqueous plant extract of *S. tuberosa* Lour and confirmed by UV-Visible analysis after 48 h. In addition, the biosynthesized AgNPs were further characterised using Zeta potential analyser, EDX, XRD, FTIR, SEM and TEM whereas the AuNPs were further characterised using EDX and SEM. The EDX analysis confirmed the presence of pure silver and gold in the respective nanoparticles. From the above results, it was confirmed that the AgNPs of *S. tuberosa* Lour were crystalline, face-centred cubic in structure and spherical in shape. From the SEM analysis, it can be known that both AgNPs and AuNPs were monodispersed. When the reduction reactions of 4-nitrophenol, methylene blue, methyl orange and methyl red in the presence of green-synthesised AgNPs were analysed in UV-Visible spectrophotometer, the absorption maximum decreased from 1.252 to 0.233, 2.480 to 0.316, 0.752 to 0.320 and 2.651 to Nil whereas in the presence of the green-synthesised AuNPs, the absorption maximum decreased from 1.252 to 0.360, 2.480 to 0.064, 3.124 to 0.134 and 0.558 to 0.117. The above results clearly indicates that the AgNPs as well as AuNPs of *S. tuberosa* Lour were acted as exhalent catalyst and degraded the abovementioned synthetic chemicals completely in the presence of $NaBH_4$.

Table 2 Absorption maxima of synthetic chemicals before and after addition of *S. tuberosa* Lour AuNPs

S. no.	Synthetic chemical	Absorption maximum	
		Before the addition of AuNPs	After the addition of AuNPs
1	4-Nitrophenol	1.252	0.360
2	Methylene blue	2.480	0.064
3	Methyl orange	3.124	0.134
4	Methyl red	0.558	0.117

Acknowledgments The authors are thankful to the University Grants Commission (UGC) RGNF's, Govt. of India, for providing financial support and the Department of Physics, Acharya Nagarjuna University, Guntur, for providing research facilities.

Compliance with ethical standards

Conflict of interest The authors declare that there is no conflict of interest.

References

Ahmed S, Ahmad M, Swami BL, Ikram S (2016) A review on plants extract mediated synthesis of silver nanoparticles for antimicrobial applications: a green expertise. J Adv Res 7(1:17–28

Ajitha B, Reddy YAK, Reddy PS (2014) Biogenic nano-scale silver particles by *Tephrosia purpurea* leaf extract and their inborn antimicrobial activity. Spectrochim Acta Part A Mol Biomol Spectrosc 121: 164–172

Ansari R, Mosayebzadeh Z, Keivani B, Mohammad-khah A (2011) Adsorption of cationic dyes from aqueous solutions using polyaniline conducting polymer as a novel adsorbent. J Adv Sci Res 2(2):27–34

Ashraf JM, Ansari MA, Khan HM, Alzohairy MA, Choi I (2016) Green synthesis of silver nanoparticles and characterization of their inhibitory effects on AGEs formation using biophysical techniques. Sci Rep 6:20414

Bharali P, Paul A, Dutta P, Gogoi G, Das AK, Baruah AM (2014) Ethnopharmacognosy of *Stemona tuberosa* Lour., a potential medicinal plant species of Arunachal pradesh, India. World J Pharm Pharm Sci 3(4):1072–1081

Edison TJI, Sethuraman MG (2013) Biogenic robust synthesis of silver nanoparticles using *Punica granatum* peel and its application as a green catalyst for the reduction of an anthropogenic pollutant 4-nitrophenol. Spectrochim Acta A Mol Biomol Spectrosc 104:262–264

Jayaseelan C, Rahuman A (2011) Acaricidal efficacy of synthesized silver nanoparticles using aqueous leaf extract of *Ocimum canum* against *Hyalomma anatolicum anatolicum* and *Hyalomma marginatum isaaci* (Acari: Ixodidae). Parasitol Res 111:1369–1378

Joseph S, Mathew B (2015) Microwave-assisted green synthesis of silver nanoparticles and their study on catalytic activity in the degradation of dyes. J Mol Liq 204:184–191

Jyoti K, Singh A (2016) Green synthesis of nanostructured silver particles and their catalytic application in dye degradation. J Genet Eng Biotechnol 14:2311–2317

Jyoti K, Baunthiyal M, Singh A (2016) Characterization of silver nanoparticles synthesized using *Urtica dioica* Linn leaves and their synergistic effects with antibiotics. J Radiat Res Appl Sci 9(3):217–227

Karthik R, Hou Y-S, Chen S-M, Elangovan A, Ganesan M, Muthukrishnan P (2016) Eco-friendly synthesis of Ag-NPs using *Cerasus serrulata* plant extract- its catalytic, electrochemical reduction of 4-NPh and antibacterial activity. J Ind Eng Chem 37:330–339

Khan S, Runguo W, Tahir K, Jichuan Z, Zhang L (2017) Catalytic reduction of 4-nitrophenol and photo inhibition of *Pseudomonas aeruginosa* using gold nanoparticles as photocatalyst. J Photochem Photobiol B Biol 170:181–187

Kharub M (2012) Use of various technologies, methods and adsorbents for the removal of dye. J Environ Res Dev 6:3A

Kjellstrom T, Lodh M, McMichael T et al (2006) Air and water pollution: burden and strategies for control. In: Jamison DT, Breman JG, Measham AR, Alleyne G, Claeson M, Evans DB, Jha P, Mills A, Musgrove P (eds) Disease control priorities in developing countries, 2nd edn. World Bank, Washington (DC), pp 817–832

Kumar TVR, Murthy JSR, Narayana Rao M, Bhargava Y (2016) Evaluation of silver nanoparticles synthetic potential of *Couroupita guianensis* Aubl., flower buds extract and their synergistic antibacterial activity. 3 Biotech 6(92)

Lee KD, Nagajyothi PC, Sreekanth TVM, Park S (2015) Eco-friendly synthesis of gold nanoparticles (AuNPs) using *Inonotus obliquus* and their antibacterial, antioxidant and cytotoxic activities. J Ind Eng Chem 26:67–72

Monali G, Jayendra K, Avinash I, Aniket G, Rai M (2009) Fungus-mediated synthesis of silver nanoparticles and their activity against pathogenic fungi in combination with fluconazole. Nanomedicine 5: 382–386

Otari SV, Patil RM, Nadaf NH, Ghosh SJ, Pawar SH (2012) Green biosynthesis of silver nanoparticles from an actinobacteria *Rhodococcus* sp. Mater Lett 72:92–94

Padalia H, Moteriya P, Chanda S (2015) Green synthesis of silver nanoparticles from marigold flower and its synergistic antimicrobial potential. Arab J Chem 8:732–741

Patra JK, Kwon Y, Baek K (2016) Green biosynthesis of gold nanoparticles by onion peel extract: synthesis, characterization and biological activities. Adv Powder Technol 27(5):2204–2213

Pei X, Qu Y, Shen W, Li H, Zhang X, Li S, Zhang Z, Li X (2017) Green synthesis of gold nanoparticles using fungus Mariannaeasp. HJ and their catalysis in reduction of 4-nitrophenol. Environ Sci Pollut Res 24:21649–21659

Prasad C, Srinivasulu K, Venkateswarlu P (2015) Catalytic reduction of 4-nitrophenol using biogenic silver nanoparticles derived from papaya (*Carica papaya*) peel extract. Ind Chem 1(1):1000104

Raja S, Ramesh V, Thivaharan V (2017) Green biosynthesis of silver nanoparticles using *Calliandra haematocephala* leaf extract, their antibacterial activity and hydrogen peroxide sensing capability. Arab J Chem 10:253–261

Reddy NKB, Kumar HAK, Mandal BK (2016) Biofabricated silver nanoparticles as green catalyst in the degradation of different textile dyes. J Environ Chem Eng 4(1):56–64

Saha J, Begum A, Mukherjee A, Kumar S (2017) A novel green synthesis of silver nanoparticles and their catalytic action in reduction of methylene blue dye. Sustain Environ Res 27:245–250

Sandeep S, Santhosh SA, Kumara Swamy N, Suresh SG, Melo SJ, Mallu P (2016) Biosynthesis of silver nanoparticles using *Convolvulus pluricaulis* leaf extract and assessment of their catalytic, electrocatalytic and phenol remediation properties. Adv Mater Lett 7(5):383–389

Shah K (2014) Biodegradation of azo dye compounds. Int Research J of Biochem and Biotech 1(2):005–013

Shanmugam C, Sivasubramanian G, Parthasarathi B, Baskaran K, Balachander R, Parameswaran VR (2016) Antimicrobial, free radical scavenging activities and catalytic oxidation of benzyl alcohol by nano-silver synthesized from the leaf extract of *Aristolochia indica* L: a promenade towards sustainability. Appl Nanosci 6:711–723

Singh S, Bharti A, Meena VK (2014) Structural, thermal, zeta potential and electrical properties of disaccharide reduced silver nanoparticles. J Mater Sci Mater Electron 25:3747–3752

Singh P, Singh H, Ju Kim Y, Mathiyalagan R, Wang C, Yang DC (2016) Extracellular synthesis of silver and gold nanoparticles by *Sporosarcina koreensis* DC4 and their biological applications. Enzym Microb Technol 86:75–83

Sinha T, Ahmaruzzaman M (2015) High-value utilization of egg shell to synthesize silver and gold–silver core shell nanoparticles and their application for the degradation of hazardous dyes from aqueous phase-a green approach. J Colloid Interface Sci 453:115–131

Sudha M, Saranya A, Selvakumar G, Sivakumar N (2014) Microbial degradation of azo dyes: a review. Int J Curr Microbiol App Sci 3(2):670–690

Supraja N, Prasad TNVKV, David E, Krishna TG (2016) Antimicrobial kinetics of *Alstonia scholaris* bark extract-mediated AgNPs. Appl Nanosci 6:779–787

Suresh G, Gunasekar PH, Kokila D, Prabhu D, Dinesh D, Ravichandran N, Ramesh B, Koodalingam A, Siva GV (2014) Green synthesis of silver nanoparticles using *Delphinium denudatum* root extract exhibits antibacterial and mosquito larvicidal activities. Spectrochim Acta Part A Mol Biomol Spectrosc 127:61–66

Suvith VS, Philip D (2014) Catalytic degradation of methylene blue using biosynthesized gold and silver nanoparticles. Spectrochim Acta A Mol Biomol Spectrosc 118:526–532

Swamy MK, Akhtar MS, Mohanty SK, Uma Rani S (2015) Synthesis and characterization of silver nanoparticles using fruit extract of *Momordica cymbalaria* and assessment of their in vitro antimicrobial, antioxidant and cytotoxicity activities. Spectrochim Acta A Mol Biomol Spectrosc 151:939–944

Syed A, Saraswati S, Kundu GC, Ahmad A (2013) Biological synthesis of silver nanoparticles using the fungus *Humicola* sp. and evaluation of their cytoxicity using normal and cancer cell lines. Spectrochim Acta Part A Mol Biomol Spectrosc 114:144–147

Tahir K, Nazir S, Li B, Ullah Khan A, UlHaq Khan Z, Yu Gong P, Ullah Khan S, Ahmad A (2015) *Nerium* oleander leaves extract mediated synthesis of gold nano- particles and its antioxidant activity. Mater Lett 156:198–201

Ul Haq Khan Z, Khan A, Chen Y, Khan A, Shah N, Muhammad N, Murtaza B, Tahir K (2017) Photo catalytic applications of gold nanoparticles synthesized by green route and electrochemical degradation of phenolic Azo dyes using AuNPs/GC as modified paste electrode. J Alloys Compd 725:869–876

Varadavenkatesan T, Selvaraj R, Vinayagam R (2016) Phyto-synthesis of silver nanoparticles from *Mussaenda erythrophylla* leaf extract and their application in catalytic degradation of methyl orange dye. J Mol Liq 221:1063–1070

Vidhu VK, Philip D (2014) Catalytic degradation of organic dyes using biosynthesized silver nanoparticles. Micron 56:54–62